nature geoscience

REVIEW ARTICLE

PUBLISHED ONLINE: 22 AUGUST 2010 | DOI: 10.1038/NGEO940

An integrated perspective of the continuum between earthquakes and slow-slip phenomena

Zhigang Peng[1]* and Joan Gomberg[2]

The discovery of slow-slip phenomena has revolutionized our understanding of how faults accommodate relative plate motions. Faults were previously thought to relieve stress either through continuous aseismic sliding, or as earthquakes resulting from instantaneous failure of locked faults. In contrast, slow-slip events proceed so slowly that slip is limited and only low-frequency (or no) seismic waves radiate. We find that slow-slip phenomena are not unique to the depths (tens of kilometres) of subduction zone plate interfaces. They occur on faults in many settings, at numerous scales and owing to various loading processes, including landslides and glaciers. Taken together, the observations indicate that slowly slipping fault surfaces relax most of the accrued stresses through aseismic slip. Aseismic motion can trigger more rapid slip elsewhere on the fault that is sufficiently fast to generate seismic waves. The resulting radiation has characteristics ranging from those indicative of slow but seismic slip, to those typical of earthquakes. The mode of seismic slip depends on the inherent characteristics of the fault, such as the frictional properties. Slow-slip events have previously been classified as a distinct mode of fault slip compared with that seen in earthquakes. We conclude that instead, slip modes span a continuum and are of common occurrence.

Slow-slip phenomena refer to specific deformation modes that are observed seismically or geodetically. The variability of slow-slip phenomena reflects a suite of unique fault-slip characteristics (Fig. 1). When faults slip at sufficiently fast velocities, dynamic forces become significant and seismic waves radiate. The energy carried at wavefronts can overcome frictional forces on locked sections of the fault, resulting in large displacements and 'fast' earthquakes[1]. Under some conditions the slip may not reach dynamic velocities, but low-amplitude, low-frequency seismic waves still radiate. These seismic slow signals have only recently been identified, facilitated by networks of high-sensitivity surface and borehole seismometers that record continuously in the frequency band of ~0.001–100 Hz. Among these signals, the most commonly observed are weak continuous vibrations having no clear impulsive phases, known as deep 'non-volcanic' tremor[2]. Tremor often accompanies the aseismic events, with the coupled phenomena named 'episodic tremor and slip' (ETS)[3].

A range of other seismic signals indicative of a spectrum of slow source durations and rupture speeds, and limited slip (relative to earthquakes), have been classified as low-frequency earthquakes (LFEs)[4,5] and very low-frequency earthquakes (VLFs)[6,7], with source durations of less than one second and a few tens of seconds, respectively (Figs 1 and 2). These weak seismic events have been observed in Japan[2], Cascadia[3], Central California[8], Mexico[9] and Costa Rica[10] (Fig. 3). In several regions where tremor signals are well recorded, a significant fraction of the tremor signal seems to comprise superposed LFE waveforms[10,11]. This implies that tremor represents the chatter from tiny, distributed sources that radiate randomly. VLFs are found buried in tremor signals, further suggesting that occasionally LFEs coalesce into an organized rupture that radiates seismic waves at a lower frequency[12,13].

Aseismic signals reflect fault slip so slow that inertial forces and seismic radiation are negligible. The occurrence of such 'quasi-static' slow slip has been known for many years (for example, ref. 14), but its significance along plate boundaries was not recognized until plate-boundary-scale GPS networks became operational in continuous mode ~15 years ago[15–17]. Less abundant strainmeters and tiltmeters also measure aseismic transients, and with much greater resolution than GPS[18].

The pervasiveness of slow-slip phenomena in plate boundary regions, the spontaneity and regularity with which they sometimes occur, and some of the seismic signals they emit are new and exciting. However, some of the phenomena have been documented for decades. Early seismological studies have shown that some earthquakes are relatively depleted of high frequencies[19], reflecting source durations longer than expected from standard relationships[20]. These include slow, mostly shallow earthquakes on oceanic transform faults[19,21] and in shallow sediments[22], tsunami earthquakes[23] and glacial earthquakes[24].

Slow-slip phenomena have also been documented in the context of other, more familiar types of fault slip. Examples include aftershocks and afterslip, repeating earthquakes and creep, swarms and various types of aseismic deformation. Although driven by gravity instead of stresses resulting from relative plate motions, glaciers and landslides also share many commonalities with slow slip of tectonic origins.

Slow-slip phenomena along tectonic plate boundary faults

When and where. The sources of the slow geodetic signals are generally consistent with shear slip on the plate interface[16,25] (Fig. 2). The locations of the slipping surface and the interface generally have uncertainties of several kilometres or more. Plate interfaces have been mapped using seismic imaging techniques, potential field methods, and high-resolution locations of earthquakes[26,27].

The most well-constrained sources of seismic slow slip (LFEs) and plate boundary locations come from the Nankai subduction zone in southwest Japan. Here, the slow-slip sources coincide with the plate boundary[26]. LFE sources in the Cascadia subduction zone[28] and along the San Andreas fault (SAF)[29] system

[1]School of Earth and Atmospheric Sciences, Georgia Institute of Technology, 311 Ferst Drive, Atlanta, Georgia 30332, USA, [2]Earthquake Hazards Program, US Geological Survey, Department of Earth and Space Sciences, University of Washington, Seattle, Washington DC 98195-1310, USA. *e-mail: zpeng@gatech.edu

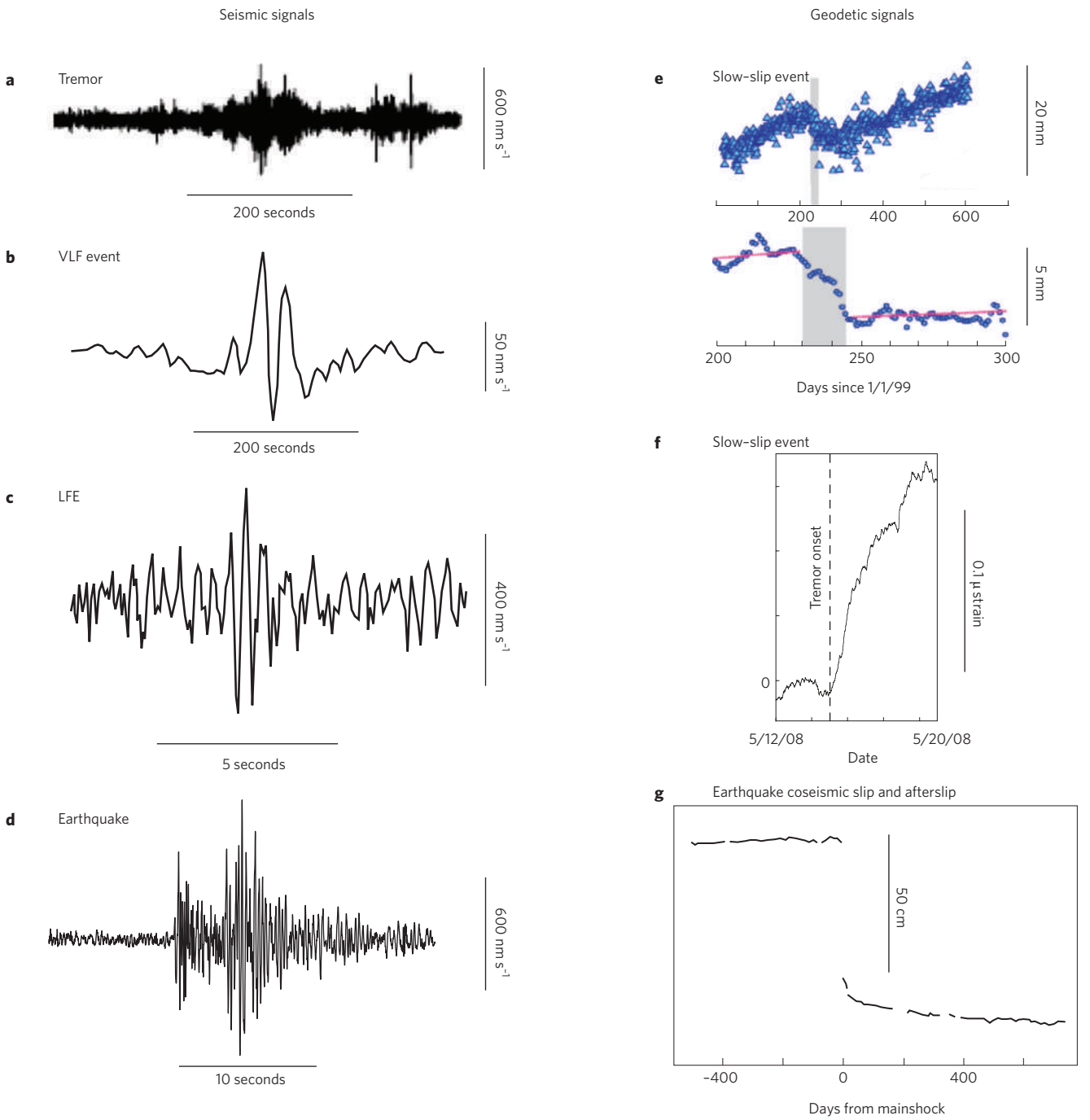

Figure 1 | Illustrative examples of slow-slip signals. a, Tremor and **b**, VLF from Japan, filtered between 2–8 and 0.005–0.05 Hz, respectively. **c**, LFE from Japan. **d**, *M*1.9 earthquake in western Washington. **e**, Top: daily GPS E–W displacements measured on Vancouver Island. Bottom: averaged and detrended GPS data (pink lines show the fit trend) reveal a slow-slip event (shaded). **f**, Slow slip in differential shear strain measured in western Washington. Strain transient onset coincides with increased tremor activity. **g**, GPS N 55° displacement ~100 km from the 2001 *M*8.4 Peru earthquake. The large offset reflects the coseismic slip and the subsequent decaying deformation may be afterslip[99]. Figures reproduced with permission from: **a**,**b** ref. 77, © 2008 GRL; **c**, ref. 5, © 2006 NPG; **e**, ref. 16, © 2001 AAAS; **f**, ref. 98, © 2008 AGU; **g**, ref. 99, © 2005 JGR.

transform boundary locate on the respective plate interfaces. A geographically broader study of LFEs in the subduction zones of Japan, Costa Rica and Cascadia also places sources on the plate interface, but samples only three-hour time windows[10]. Slip vectors estimated from LFEs and VLFs in Japan indicate slip along the plate interface in the convergence direction[13,30].

In Cascadia, quasi-static slip of several centimetres on the plate interface has been inferred directly downdip from the locked zone of the plate interface, between the 25- and 45-km-depth contours[16]. However, the non-uniqueness of the modelled solutions also permits slip zones at different depths or shear distributed over a depth range of more than 10 km (ref. 31). In much of Cascadia, tremor sources are consistent with origins on the plate interface[10,28], but their distribution beneath Vancouver Island extends from the plate interface to near the surface with the densest concentration being well above the interface[31,32].

The durations of aseismic-slip events in numerous subduction zones range from days to years, with magnitudes of displacement

of up to several tens of centimetres[31,33]. In Japan and Cascadia these events occur quasi-periodically, with periods of ~3 to ~19 months that vary along each subduction zone[3,25,34,35]. Elsewhere, for example Alaska, Mexico, New Zealand and Costa Rica, slow-slip events sometimes recur but with no apparent regularity[17,36,37].

Quasi-static-slip events are accompanied by a variety of seismic phenomena. In many regions where aseismic slip occurs beneath the locked zone, for example Cascadia and southwest Japan, tremor always accompanies quasi-static slip. However, the converse is not true, for the reasons noted below[3,25,38]. A few studies in Japan note that aseismic slip begins before the onset of tremor activity and, in some places, occurs without any detectable seismic signals[39,40].

Aseismic slip at shallow depths has correlative seismic signals that have spectral and scaling characteristics more typical of ordinary 'fast' earthquakes. Examples include regions just downdip of the shallow slow-slipping zones of the subduction zones of northern New Zealand[41] and the Boso peninsula, Japan[42]. Shallow quasi-static slip accompanied by increased rates of regular earthquakes has also been observed along the creeping section of the SAF[14] and the south flank of the Kilauea volcano, Hawaii[43]. The coupled earthquakes locate where ambient seismicity occurs, beneath the zone of quasi-static slip.

Seismic slow-slip signals observed without geodetic counterparts, such as along the SAF[29,44,45] and in the subduction zones noted above, plausibly can be attributed to detection differences between geodetic and seismic instrumentation. Such differences between regions may explain some apparent regional variations in slow-slip phenomena. Surface GPS instruments are sensitive only to quasi-static-slip events below ~25 km depth with magnitude (M) > 6, whereas small M5–6 events can be detected only by borehole tiltmeters in Japan[25]. Even with borehole strainmeters, M~5 slow-slip events could go undetected if at depths below ~15 km[45]. The observation of tremor both during ETS events and between them suggests that quasi-static slip may often occur between such events but go undetected[40,46]. On the other hand, deep ETS events have been measured in southwest Japan[47], but have not been observed directly in northeast Japan, yet both regions contain equally dense seismic and geodetic instrumentation.

Shear slip on frictional, pressurized, near-failure faults. Numerous lines of evidence strongly suggest that slow-slip phenomena result from shear slip on faults near failure with low effective confining pressure, most probably owing to near-lithostatic fluid pressures. Tremor in a wide range of tectonic environments can be instantaneously triggered by transient stresses on the order of a few to tens of kilopascals, imparted by surface waves of regional and teleseismic events[44,48–51] (Fig. 4). Static-stress changes on the order of a few kilopascals from neighbouring earthquakes also trigger changes in rates of tremor[52] and LFEs[29] along the SAF. Furthermore, tremor activity seems to be modulated by the Earth's tidal deformation[53–55], with tidally induced fault-parallel shear stresses correlating best with the tremor activity[56]. Correlations between slow-slip phenomena and stress perturbations on the order of a few kilopascals from atmospheric[57] and other climatic-driven events[58,59] also indicate that participating faults are critically stressed.

It is generally agreed that near-lithostatic fluid pressure reduces the effective stresses and makes slow-slip events highly sensitive to external stress perturbations. Evidence of elevated fluid pressures comes from tomographic imaging of elastic properties around the source region of the slow-slip phenomena[5,27,60–62]. These studies show that tremor and aseismic slip occur preferentially in regions with high ratios of compressional- to shear-wave seismic velocity, anomalously high Poisson's ratios, or ultralow shear-velocity layers. These all indicate that fluids are widely present, with pore pressures near lithostatic values (Fig. 2). Fluids may come from dehydration of hydrous minerals in the subducting sediments and oceanic crust[63],

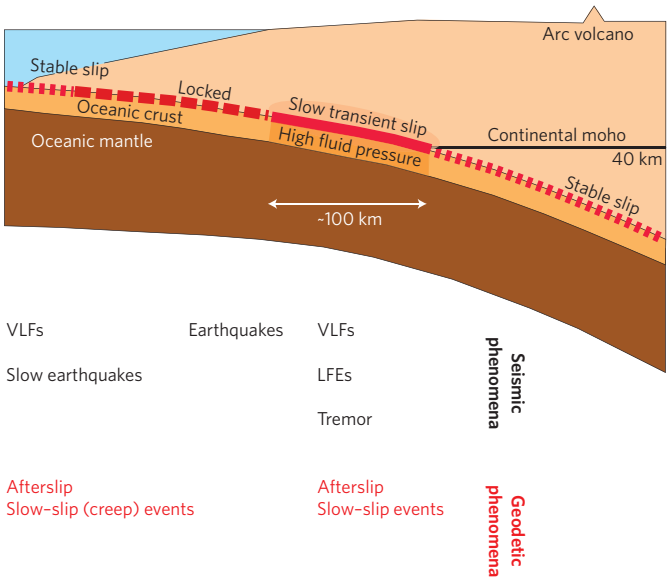

Figure 2 | Schematic cross-section of the Cascadia subduction zone. The various slip modes believed to occur along the plate interface are noted (red lines) with the corresponding observed phenomena indicative of each listed below. In Cascadia and elsewhere much evidence suggests that high fluid pressures exist in the region where slow-slip phenomena occur. Modified from ref. 61, © 2009 NPG, ref. 5, © 2006 NPG and ref. 62, © 2009 AAAS.

becoming sealed in and pressurized where the plate boundary has low permeability[27,61]. The presence and source of fluids in the lower crust near strike-slip faults such as the SAF are still speculative, although recent seismic imaging studies have revealed conductive properties at the base of the crust[64].

Physical models of slow-slip phenomena. The macroscopic behaviours of plate boundary faults under the stresses caused by relative plate motions are typically described in terms of frictional properties[65]. Thus, most models of aseismic slow-slip events appeal to shear slip on frictional faults[5,30,50]. Figure 2 illustrates the broad variation in frictional properties that are ascribed to subduction zones, but applicable to several plate boundary zones. The same picture can be drawn for transform boundaries by simply plotting the interface vertically[66]. Frictional models explain the occurrence of quasi-static-slip events with rates and displacement values consistent with observations[67–71], although the physics assumed in these models may differ. Moreover, they seem to require low confining stresses and, in some models, significant involvement of fluid-pressure processes[71], consistent with the aforementioned inferences.

Other explanatory models involve fluids, either exclusively through mechanisms such as hydraulic fracturing or permeability pumping[2,32], or in combination with frictional processes[49,70,71]. An intriguing example of the latter involves dilatant strengthening. Here, frictional faults dilate as they accelerate towards dynamic failure at rates that prohibit draining, such that pore pressures drop. This raises the effective normal stress and thus limits or quenches dynamic rupture[70,71]. The lack of phase lag between seismic waves and tidal forces, the tremor and slip rates they modulate, and high tremor-migration rates (as high as 5–45 km hr^{-1} (ref. 11), in excess of plausible fluid-diffusion rates) imply that changing fluid pressures cannot involve diffusion or flow[72].

A primary role for quasi-static slip. The earliest ETS observations clearly demonstrated the coupled nature of seismic and aseismic slow-slip events[3]. Corroborative subsequent studies have led to

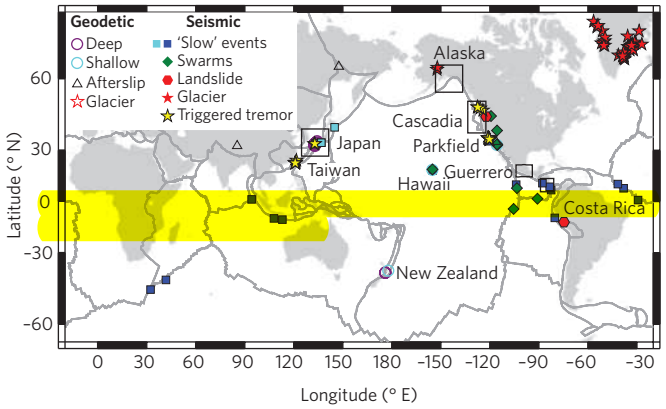

Figure 3 | Location map of seismically and geodetically observed slow-slip phenomena. Regions where ETS events have been observed are marked by black boxes. Modified from ref. 47, © 2007 AGU and ref. 100, © 2010 Springer. The locations of some slow-slip phenomena for which measurements of duration and moment have been made and plotted in Fig. 5 are shown with the same symbols (see Supplementary Table 1). The yellow stars mark the locations of tremor triggered by regional and teleseismic earthquakes[44,48–51].

proposals that tremor could be used as a proxy to monitor aseismic slip[29,38,73]. As well as the broadscale temporal and spatial coincidence of seismic (tremor, LFE and VLF) and quasi-static-slip sources within tens of kilometres and days, in Cascadia and Japan both also show clear along-strike migrations that track each other, at speeds on the order of a few tens of kilometres per day[12,46]. These correlations warrant exploration of a causal connection between the seismic and aseismic phenomena. 'Causal' in this context refers both to the processes that load or supply the strain energy fuelling the eventual fault slip, and those that may initiate (trigger) a slip event early. The relative timing and moments of seismic and aseismic slow slip provide key constraints on the driving and triggering processes. The moment measures the potency of a slip episode to relax accrued stresses, and is proportional to the product of the slipping area and the distance slipped[74].

Although resolvable in only a few cases, the fact that the onset of aseismic slip precedes the start of the seismic activity in Hawaii[43] and Japan[39,40] means the seismic slip does not trigger the quasi-static slip. However, the reverse may be inferred. We also conclude that the seismic slip is not causal in the sense of providing the energy that drives the aseismic slip, because when measurable, the relative moment of the cumulative seismic activity is orders of magnitude smaller than that of the aseismic slip (Fig. 5). In Japan, aseismic-slip events near the Boso peninsula region have moments that significantly exceed those of the earthquakes that accompany them[42]. In the Nankai region the rate of seismic moment released from detectable VLF sources was 0.1% of the rates from adjacent, contemporary slow-slip events[13]. In Cascadia, for each of eight ETS episodes the moment of the aseismic slip exceeds that of the cumulative tremor by more than a factor of a million[75]. Tremor represents only the energy radiated above ~1 Hz, thus the latter probably underestimates the total seismic moment. Indeed, coherent seismic waveforms with energy at frequencies as low as 0.002 Hz have been observed in association with aseismic-slip events, but always in the tremor signals[12,76]. This demonstrates the detectability of such low-frequency radiation and shows that biases in band-limited estimates of seismic moment are probably too small to account for their much smaller values relative to aseismic moments.

Thus, we conclude that quasi-static slip is the primary mode in which the accrued tectonic stresses are relieved. The observations do not distinguish between the seismic slip also being tectonically driven or relaxing stresses redistributed as a result of the aseismic slip. Although uncertain, the possible balance between the cumulative aseismic slip over complete ETS cycles and that accrued owing to plate motion in Cascadia would argue in favour of the first proposition[46,77].

Slip-mode stationarity. We suggest that the specific slip mode at a particular location is an inherent property of the fault, rather than being determined by transient conditions (for example, the causative load itself, or fluid flow). The observation of only a single mode of slip at a given locale for the duration of our observational window of several decades supports this inference, and further implies that the properties governing the slip mode are stationary on this timescale. Corroborative observations include spatially anticorrelated distributions of earthquakes and slow-slip sources, observed for both large and small earthquakes. Sources of slow quasi-static slip in Alaska abut the rupture zone of the great *M*9.2 Alaska earthquake[78] of 1964. In Japan, slow-slip sources occur on the edges of the rupture planes of the *M*7.9 Kanto earthquake[42] of 1923 and just below the *M*7.9 Tonankai 1944 and *M*8.0 Nankai 1946 earthquakes[79]. In Cascadia, the locations of tremor sources are anticorrelated with the section of the plate interface inferred from palaeoseismic data to have slipped during past megathrust earthquakes[76] and, curiously, also with earthquakes in the crust of the overriding plate[31].

The maxima of seismic and aseismic slow-slip source distributions also seem to locate in spatially adjacent, but not coincident, regions. The most recent estimates of tremor and quasi-static slow slip from Japan show the two migrating in temporal sync with one another, but with a bimodal tremor distribution that has peaks outlining the slower slip rather than being coincident with it[80]. Tremor source distributions mapped in the subduction zone regions of Mexico, Alaska and Cascadia all peak downdip of the greatest quasi-static slip[31,36,62].

Conditions for slow-slip phenomena. Although the mode of slip seems to be stationary, the requirements for triggering slip vary temporally and are not easily satisfied. Recent systematic surveys of tremor in California[44,48] and Taiwan[51], triggered by the seismic waves from distant earthquakes, revealed that triggered tremor occurs in only a few isolated regions, the locations of which varied for different triggering earthquakes.

The particular conditions required for slow slip have become apparent as more regions have been studied. Thermal controls were initially thought to be key[47] because ETS was first identified in the relatively young and warm subducted crusts of Cascadia and southwest Japan, and were absent in northeast Japan where the predicted pressure–temperature paths are much cooler[63]. However, detailed finite-element thermal modelling of the Cascadia and southwest Japan subduction zones now shows quite different pressure–temperature paths in each region at depths where ETS is observed, suggesting that ETS does not require a specific temperature or metamorphic reaction[81]. Furthermore, tremor and slow-slip events have been recently observed in relatively old and cold subducting crust in Costa Rica[10] and Alaska[36]. Hence new hypotheses invoking differences in frictional or permeability properties have been proposed to explain the lack of ETS in northeast Japan[47,63]. However, more work is required to fully test these hypotheses.

Slow-slip phenomena in a larger context

Coupled seismic- and aseismic-slip events on natural surfaces have been observed in many contexts, some fairly familiar and well studied. As just noted in the context of the newly discovered plate boundary phenomena, investigations in many

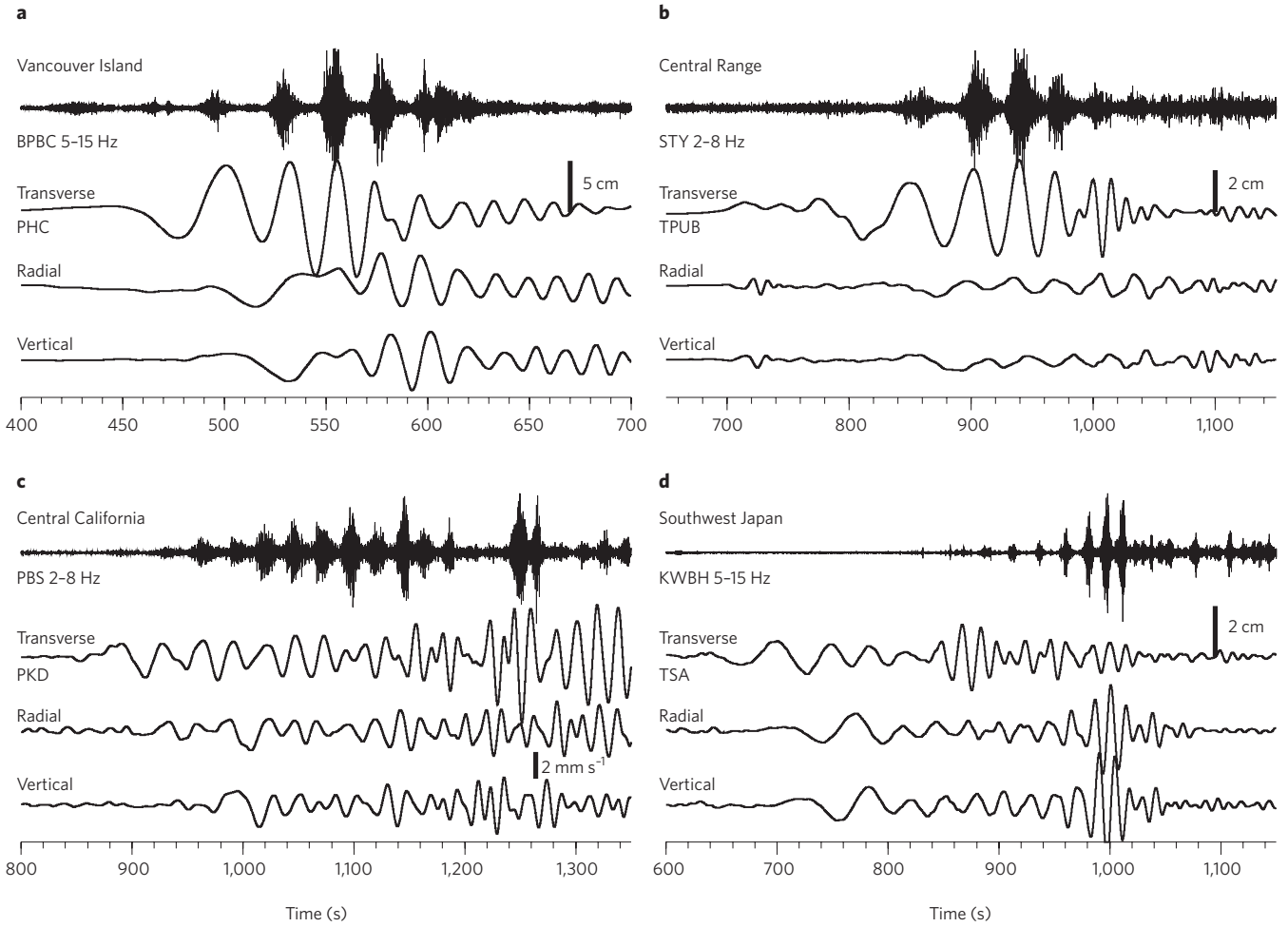

Figure 4 | Examples of triggering seismic waves and triggered tremor. A comparison of surface waves of large teleseismic earthquakes and triggered tremor beneath **a**, Vancouver Island in British Columbia, **b**, the Central Range in Taiwan, **c**, the SAF in Central California and **d**, the subduction zone in southwest Japan. The station and component names and the frequency ranges of the applied filters are marked on the left-hand side of the traces. The traces have been time-shifted to reflect the relationship between the surface waves and tremor at the source region. Figures reproduced with permission from: **a**, ref. 50, © 2007 NPG; **b**, ref. 51, © 2008 GJI; **c**, ref. 44, © 2009 GJI; **d**, ref. 49, © 2008 EPS.

settings are required to learn which factors are most relevant and provide opportunities to fill in observational gaps that arise from instrumental limitations in individual settings. We identify at least five hallmark characteristics of slow-slip phenomena: (1) the ratios of slip to slipped area are low and durations are long, relative to 'fast' earthquakes; (2) accrued stresses are relaxed dominantly through quasi-static slip that triggers a seismic response, evident in aseismic slip that precedes the seismic activity and has greater moment. The seismic response is sometimes quenched before reaching fully dynamic speeds, as in tremor, LFEs and VLFs; (3) explanatory models invoke shear slip on faults with frictional properties transitional between those that result in continuous creep and those that are fully locked, punctuated by nearly instantaneous slip (stick–slip); (4) near-failure conditions probably reflect low confining stresses. Fluids at high pressure remain the most viable way to achieve these conditions, and may play important roles in quenching slip and in the recurrence of slow-slip events; (5) local, stationary properties determine the dominant slip mode.

Afterslip and aftershocks. Afterslip represents transient quasi-static slip triggered by the rapid stress release in a mainshock, which is typically followed by increased seismic activity known as 'aftershocks'. The underlying mechanism of aftershock generation is still debated[82]. A linear relationship between postseismic geodetic deformation, modelled as slow slip on the mainshock fault, and the cumulative number of aftershocks has led to suggestions that aftershocks may be driven primarily by afterslip[83–85]. These coupled seismic and aseismic processes exhibit almost all of the aforementioned hallmark characteristics of slow-slip phenomena: (1) the durations of the aseismic slip and aftershock sequences may last for days to months; (2) the afterslip moment exceeds the aggregate moment of aftershocks by more than two orders of magnitude (Fig. 5)[85,86]; (3) frictional models akin to those applied to tectonically driven plate boundary slow slip explain not only the temporal decay of aftershocks and afterslip, but also their spatial migration[87,88]; (4) anti-correlated coseismic- and postseismic-slip distributions suggest that afterslip fills in gaps in slip remaining after a mainshock[84].

Aseismic deformation and earthquake swarms. Sometimes sequences of clustered earthquakes strike in a short period of time with no obvious mainshock. The driving forces for these 'earthquake swarms' may be aseismic slip (measured in just a few cases), fluid, or magma migrations[43,72,89,90]. Swarms share several key features with plate boundary slow-slip phenomena[72]: (1) durations of swarm activity and aseismic slip last days to months; (2) the aggregate seismic moment is only a small fraction of the cumulative

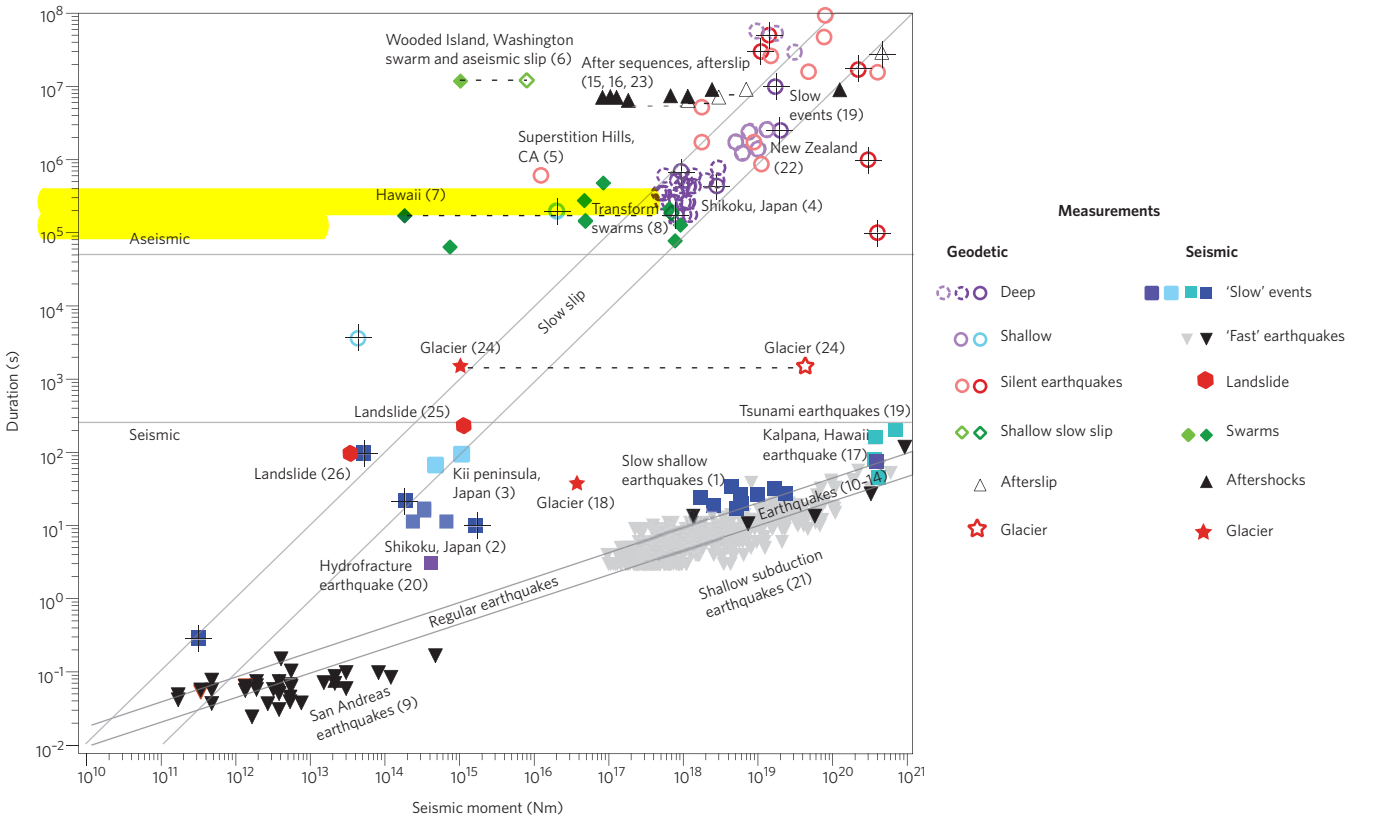

Figure 5 | Seismic moment versus source duration for a variety of fault-slip observations. Augmented version from ref. 96, © 2007 NPG, which infers two distinct scalings between moment and duration (diagonal bands). Open and filled symbols denote geodetic and seismic measurements, respectively. Measurements from ref. 96 have plus signs on the symbols, and all others are cross-referenced to sources listed in Supplementary Table S1. 'Fast earthquakes' and 'shallow subduction earthquakes' are too numerous to list but are listed in Supplementary Table S1. Data from the former come from only two sources. Dashed horizontal lines connect related geodetic and seismic data. Solid horizontal lines highlight the gap between seismic and geodetic durations.

aseismic moment[90] (Fig. 5) and some swarm events migrate at rates of kilometres per hour, consistent with the propagation of slow-slip events[72]; (3) the magnitudes of swarm earthquakes tend to be small and irregularly distributed in a sequence, reminiscent of tremor activity; (4) pressurized fluids are often invoked in explanations of swarms in magmatic and geothermal environments; (5) in the case of Hawaiian swarms, the earthquakes occurred in the same region as background seismicity[43].

Steady and transient fault creep and repeating earthquakes. Sections of the SAF[91] and other principal plate boundary faults around the globe[42] are known to creep steadily or exhibit transient aseismic slip. These often have associated seismic activity. 'Repeating earthquakes' are one example and probably represent repeated seismic failure of a single strongly coupled spot loaded by aseismic creep on the surrounding fault plane[91]. Other sections of the SAF are characterized by occasional transient aseismic-slip events, some of which are accompanied by increased seismicity rates[14], and others without any seismic response[92]. These coupled aseismic and seismic phenomena share the aforementioned distinguishing characteristics: (1) the transient aseismic slip lasts days to weeks[14,92]; (2) the aggregate moment release from the triggered earthquakes is negligible compared with that from the slow-slip events[14]; (3) although the materials and conditions may differ, the same frictional models and input parameters invoked to explain deeper plate boundary slow slip have been applied to explain shallow, steady and transient slip[87]; (4) high pore pressures are inferred to be responsible for the creep and transient slip[92]; (5) triggered earthquakes occur in the same regions as ambient seismicity[14].

Gravity-driven aseismic and seismic slip. Landslides and glaciers occur on natural surfaces that move and exhibit many of the same behaviours as tectonic faults, including coupled seismic and aseismic slip: (1) slip is sufficiently slow that even the seismic radiation may have characteristics typical of slow tectonic events; (2) although simultaneous geodetic and seismic measurements have been made in only a few glacier studies, results indicate that the aseismic slip triggers the seismic motion and is the primary mode of relaxing the stored gravitational energy. A slip event on an Antarctic glacier has a geodetic moment that exceeds the seismic moment by orders of magnitude (Fig. 5), and the arrival time of the first seismic energy, corrected for the source-receiver travel time, lags the onset of geodetically estimated slip by 20–150 seconds[93]; (3) glacial quakes in Antarctica, Alaska and Greenland have been interpreted as frictional stick–slip behaviour at the base of ice masses[24]. A more detailed geodetic and seismic study of an Antarctic glacier infers dynamic slip on frictionally strong spots that radiate on an otherwise quasi-statically sliding basal surface[93]; (4) pore-pressure evolution plays a significant role both in landslide and glacier movements. Theoretical models of landslide movement by stable and stick–slip sliding involve coupled frictional and pore-pressure diffusion processes[94]. Correlations between landslide velocities and diurnal changes in atmospheric pressure have been attributed to pore-pressure-diffusion processes that modulate basal pore pressure and thus the shear strength and velocity[95]. Weakening resulting

from pore-pressure changes associated with seasonal variations in water availability has been postulated to be responsible for a greater rate of glacial quakes during the summer months in Greenland[24].

A continuum of slip modes?

The fault surface we propose primarily slips quasi-statically, such that the amplitude and rate of slip are limited, perhaps because the fault surfaces are inherently weak or the failure process becomes quenched. This slow slip probably involves intermediate frictional processes between stick–slip behaviour and steady creep that result in the nucleation of failure or slip, and other processes involving fluid pressures that may quench the acceleration of slip (for example, dilatant hardening). Scattered on or near this fault surface are tiny fault patches that may accelerate to dynamic or near-dynamic rupture velocities and radiate seismic waves.

The time required for slip events of particular efficacy to completely release accrued stresses can be quantified in terms of the scaling between duration and moment. This scaling is diagnostic of the underlying mechanics. We hypothesize that slip modes observed in nature should span a continuum, given the heterogeneity and complexity of natural systems, rather than separating neatly into distinct fast or slow groups, as has been suggested[96]. We test this hypothesis by augmenting the plot of moment versus duration observations that led to the latter conclusion, with measurements from the broader range of sources described herein (Fig. 5). We plot the aggregate durations and moments for aftershock and swarm sequences as proxies for aseismic slip, noting that the aseismic moments are likely to be much larger and thus would be within the distribution of the other slow geodetic measurements. The few swarms and aftershock sequences for which both seismic and geodetic observations (connected by dashed lines) exist support this assumption.

The augmented scaling data suggest a more careful consideration of the existence of two distinct failure modes — fast and slow. Two distributions clearly exist in the data, but we suggest that they are observational, comprising either geodetic or seismic measurements. These are separated by a gap in duration of more than two orders of magnitude (Fig. 5, horizontal lines). This gap may be attributed partly to instrumental limitations[18]. It is reasonable to question whether the slow-scaling relation originally inferred even fits this larger dataset, as well as the validity of fitting a single line to widely separated clusters of data. We suggest that as more data are added, the lines separating slow- and fast-slip events will blur even more, indicating a continuum of slip modes.

Measurements of earthquakes and slow-slip events from a broad range of global settings are found to overlap with measurements of slow-slip events at plate boundary settings (Fig. 5). This overlap implies that the recently discovered slow-slip phenomena, generated at plate boundaries as a result of tectonic processes, are not so extraordinary. Furthermore, we suggest that a continuum of slip modes exists, rather than the distinct separation between slow slip and earthquakes. The mode of slip is determined by the inherent properties of the fault surface. Studies of slow-slip phenomena, viewed from a global, integrated perspective, are leading to a more complete picture of how faults slip and release tectonic stresses. Such an integrated perspective is critical for evaluating the hazards posed by earthquakes and other natural systems involving catastrophic slip. For example, it has been suggested that slow-slip phenomena could be used to delineate the updip and downdip limits of the seismogenic zone that ruptures in megathrust earthquakes[76]. Slow slip also imparts stress changes on nearby locked faults and may act as a trigger for large earthquakes, although robust observations of this process are rare[97]. The strong sensitivity of slow-slip phenomena to stress perturbations suggests that they could serve as natural 'stress meters' to monitor fault zones during large earthquake cycles.

References

1. Brodsky, E. E. & Mori, J. Creep events slip less than ordinary earthquakes. *Geophys. Res. Lett.* **34,** L16309 (2007).
2. Obara, K. Nonvolcanic deep tremor associated with subduction in southwest Japan. *Science* **296,** 1679–1681 (2002).
3. Rogers, G. & Dragert, H. Episodic tremor and slip on the Cascadia subduction zone: The chatter of silent slip. *Science* **300,** 1942–1943 (2003).
4. Katsumata, A. & Kamaya, N. Low-frequency continuous tremor around the Moho discontinuity away from volcanoes in the southwest Japan. *Geophys. Res. Lett.* **30,** 1020 (2003).
5. Shelly, D. R., Beroza, G. C. & Ide, S. Low-frequency earthquakes in Shikoku, Japan, and their relationship to episodic tremor and slip. *Nature* **442,** 188–191 (2006).
6. Obara, K. & Ito, Y. Very low frequency earthquakes excited by the 2004 off the Kii peninsula earthquakes: A dynamic deformation process in the large accretionary prism. *Earth Planets Space* **57,** 321–326 (2005).
7. Ito, Y., Asano, Y. & Obara, K. Very low-frequency earthquakes indicate a transpressional stress regime in the Nankai accretionary prism. *Geophys. Res. Lett.* **36,** L20309 (2009).
8. Nadeau, R. M. & Dolenc, D. Nonvolcanic tremors deep beneath the San Andreas Fault. *Science* **307,** 389 (2005).
9. Payero, J. S. *et al.* Nonvolcanic tremor observed in the Mexican subduction zone. *Geophys. Res. Lett.* **35,** L07305 (2008).
10. Brown, J. R. *et al.* Deep low-frequency earthquakes in tremor localize to the plate interface in multiple subduction zones. *Geophys. Res. Lett.* **36,** L19306 (2009).
11. Shelly, D. R, Beroza, G. C. & Ide, S. Non-volcanic tremor and low-frequency earthquake swarms. *Nature* **446,** 305–307 (2007).
12. Ito, Y., Obara, K., Shiomi, K., Sekine, S. & Hirose, H. Slow earthquakes coincident with episodic tremors and slow slip events. *Science* **315,** 503–506 (2007).
13. Ito, Y., Obara, K., Matsuzawa, T. & Maeda, T. Very low frequency earthquakes related to small asperities on the plate boundary interface at the locked to aseismic transition. *J. Geophys. Res.* **114,** B00A13 (2009).
14. Linde, A. T., Gladwin, M., Johnston, M., Gwyther, R. & Bilham, R. A slow earthquake sequence on the San Andreas Fault. *Nature* **383,** 65–68 (1996).
15. Hirose, H., Hirahara, K., Kimata, F., Fujii, N. & Miyazaki, S. A slow thrust slip event following the two 1996 Hyuganada earthquakes beneath the Bungo Channel, southwest Japan. *Geophys. Res. Lett.* **26,** 3237–3240 (1999).
16. Dragert, H., Wang, K. & James, T. S. A silent slip event on the deeper Cascadia subduction interface. *Science* **292,** 1525–1528 (2001).
17. Lowry, A. R., Larson, K. M., Kostoglodov, V. & Bilham, R. Transient fault slip in Guerrero, southern Mexico. *Geophys. Res. Lett.* **28,** 3753–3756 (2001).
18. Agnew, D. Instrumental, theoretical, temporal, and statistical challenges in the search for transient deformations. *Eos* **90** (suppl.), G32A-01 (2009).
19. Beroza, G. & Jordan, T. Searching for slow and silent earthquakes using free oscillations. *J. Geophys. Res.* **95,** 2485–2510 (1990).
20. Kanamori, H. & Anderson, D. L. Theoretical basis of some empirical relations in seismology. *Bull. Seismol. Soc. Am.* **65,** 1073–1095 (1975).
21. Shearer, P. M. Global seismic event detection using a matched filter on long-period seismograms. *J. Geophys. Res.* **99,** 13713–13725 (1994).
22. Kanamori, H. & Hauksson, E. A slow earthquake in the Santa Maria Basin, California. *Bull. Seismol. Soc. Am.* **82,** 2087–2096 (1992).
23. Kanamori, H. & Kikuchi, M. The 1992 Nicaragua Earthquake - a slow tsunami earthquake associated with subducted sediments. *Nature* **361,** 714–716 (1993).
24. Ekström, G., Nettles, M. & Abers, G. A. Glacial earthquakes. *Science* **302,** 622–624 (2003).
25. Obara, K., Hirose, H., Yamamizu, F. & Kasahara, K. Episodic slow slip events accompanied by non-volcanic tremors in southwest Japan subduction zone. *Geophys. Res. Lett.* **31,** L23602 (2004).
26. Shelly, D. R., Beroza, G. C., Zhang, H., Thurber, C. H. & Ide, S. High-resolution subduction zone seismicity and velocity structure beneath Ibaraki Prefecture, Japan. *J. Geophys. Res.* **111,** B06311 (2006).
27. Audet, P., Bostock, M. G., Boyarko, D. C., Brudzinski, M. R. & Allen, R. M. Slab morphology in the Cascadia forearc and its relation to episodic tremor and slip. *J. Geophys. Res.* **115,** B00A16 (2010).
28. LaRocca, M. *et al.* Cascadia tremor located near the plate interface constrained by S minus P wave times. *Science* **323,** 620–623 (2009).
29. Shelly, D. R. Migrating tremors illuminate complex deformation beneath the seismogenic San Andreas Fault. *Nature* **463,** 648–653 (2010).
30. Ide, S., Shelly, D. R. & Beroza, G. C. Mechanism of deep low frequency earthquakes: Further evidence that deep non-volcanic tremor is generated by shear slip on the plate interface. *Geophys. Res. Lett.* **34,** L03308 (2007).
31. Kao, H., Shan, S-J., Dragert, H. & Rogers, G. Northern Cascadia episodic tremor and slip: A decade of tremor observations from 1997 to 2007. *J. Geophys. Res.* **114,** B00A12 (2009).
32. Kao, H. *et al.* A wide depth distribution of seismic tremors along the northern Cascadia margin. *Nature* **436,** 841–844 (2005).

33. Miyazaki, S., Segall, P., McGuire, J. J., Kato, T. & Hatanaka, Y. Spatial and temporal evolution of stress and slip rate during the 2000 Tokai slow earthquake. *J. Geophys. Res.* **111,** B03409 (2006).
34. Miller, M. M., Melbourne, T., Johnson, D. J. & Sumner, W. Q. Periodic slow earthquakes from the Cascadia subduction zone. *Science* **295,** 2423 (2002).
35. Brudzinski, M. R. & Allen, R. M. Segmentation in episodic tremor and slip all along Cascadia. *Geology* **35,** 907–910 (2007).
36. Peterson, C. L. & Christensen, D. H. Possible relationship between nonvolcanic tremor and the 1998–2001 slow-slip event, south central Alaska. *J. Geophys. Res.* **114,** B06302 (2009).
37. Douglas, A., Beavan, J., Wallace, L. & Townend, J. Slow slip on the northern Hikurangi subduction interface, New Zealand. *Geophys. Res. Lett.* **32,** 1–4 (2005).
38. Aguiar, A. C., Melbourne, T. I. & Scrivner, C. W. Moment release rate of Cascadia tremor constrained by GPS. *J. Geophys. Res.* **114,** B00A05 (2009).
39. Fukuda, M., Sagiya, T. & Asai, Y. A causal relationship between the slow slip event and deep low frequency tremor indicated by strain data recorded at Shingu borehole station. *Eos* **89** (suppl.), U33A-0033 (2008).
40. Obara, K. Phenomenology of deep slow earthquake family in southwest Japan: Spatiotemporal characteristics and segmentation. *J. Geophys. Res.* doi:10.1029/2008JB006048 (2010).
41. Delahaye, E. J., Townend, J., Reyners, M. E. & Rogers, G. Microseismicity but no tremor accompanying slow slip in the Hikurangi subduction zone, New Zealand. *Earth Planet. Sci. Lett.* **277,** 21–28 (2009).
42. Kimura, H., Kasahara, K. & Takeda, T. Subduction process of the Philippine Sea Plate off the Kanto district, central Japan, as revealed by plate structure and repeating earthquakes. *Tectonophysics* **472,** 18–27 (2009).
43. Segall, P., Desmarais, E., Shelly, D., Miklius, A. & Cervelli, P. Earthquakes triggered by silent slip events on Kilauea volcano, Hawaii. *Nature* **442,** 71–74 (2006).
44. Peng, Z., Vidale, J. E., Wech, A. G., Nadeau, R. M. & Creager, K. C. Remote triggering of tremor along the San Andreas Fault in central California. *J. Geophys. Res.* **114,** B00A06 (2009).
45. Smith, E. F. & Gomberg, J. A search in strainmeter data for slow slip associated with triggered and ambient tremor near Parkfield, California. *J. Geophys. Res.* **114,** B00A14 (2009).
46. Wech, A. G., Creager, K. C. & Melbourne, T. I. Seismic and geodetic constraints on Cascadia slow slip. *J. Geophys. Res.* **114,** B10316 (2009).
47. Schwartz, S. Y. & Rokosky, J. M. Slow slip events and seismic tremor at circum-pacific subduction zones. *Rev. Geophys.* **45,** RG3004 (2007).
48. Gomberg, J., Rubinstein, J. L., Peng, Z., Creager, K. C. & Vidale, J. E. Widespread triggering of non-volcanic tremor in California. *Science* **319,** 173 (2008).
49. Miyazawa, M. & Brodsky, E. E. Deep low-frequency tremor that correlates with the passing surface waves. *J. Geophys. Res.* **113,** B01307 (2008).
50. Rubinstein, J. L. *et al.* Non-volcanic tremor driven by large transient shear stresses. *Nature* **448,** 579–582 (2007).
51. Peng, Z. & Chao, K. Non-volcanic tremor beneath the Central Range in Taiwan triggered by the 2001 Mw7.8 Kunlun earthquake. *Geophys. J. Int.* **175,** 825–829 (2008).
52. Nadeau, R. M. & Guilhem, A. Nonvolcanic tremor evolution and the San Simeon and Parkfield, California, earthquakes. *Science* **325,** 191–193 (2009).
53. Rubinstein, J. L., La Rocca, M., Vidale, J. E., Creager, K. C. & Wech, A. G. Tidal modulation of nonvolcanic tremor. *Science* **319,** 186–189 (2008).
54. Nakata, R., Suda, N. & Tsuruoka, H. Non-volcanic tremor resulting from the combined effect of Earth tides and slow slip events. *Nature Geosci.* **1,** 676–678 (2008).
55. Lambert, A., Kao, H., Rogers, G. & Courtier, N. Correlation of tremor activity with tidal stress in the northern Cascadia subduction zone. *J. Geophys. Res.* **114,** B00A08 (2009).
56. Thomas, A. M., Nadeau, R. M. & Bürgmann, R. Tremor-tide correlations and near-lithostatic pore pressure on the deep San Andreas fault. *Nature* **462,** 1048–1051 (2009).
57. Liu, C-C., Linde, A. T. & Sacks, I. S. Slow earthquakes triggered by typhoons. *Nature* **459,** 833–836 (2009).
58. Shen, Z. K., Wang, Q., Bürgmann, R. & Wan, Y. Pole-tide modulation of slow slip events at circum-Pacific subduction zones. *Bull. Seismol. Soc. Am.* **95,** 2009–2015 (2005).
59. Lowry, A. R. Resonant slow fault slip in subduction zones forced by climatic load stress. *Nature* **442,** 802–805 (2006).
60. Matsubara, M., Obara, K. & Kasahara, K. High-VP/VS zone accompanying non-volcanic tremors and slow-slip events beneath southwestern Japan. *Tectonophysics* **472,** 6–17 (2009).
61. Audet, P., Bostock, M. G., Christensen, N. I. & Peacock, S. M. Seismic evidence for overpressured subducted oceanic crust and megathrust fault sealing. *Nature* **457,** 76–78 (2009).
62. Song, T. A. *et al.* Subducting slab ultra-slow velocity layer coincident with silent earthquakes in southern Mexico. *Science* **324,** 502–506 (2009).
63. Peacock, S. M. Thermal and metamorphic environment of subduction-zone episodic tremor and slip. *J. Geophys. Res.* **114,** B00A07 (2009).
64. Ozacar, A. A. & Zandt, G. Crustal structure and seismic anisotropy near the San Andreas Fault at Parkfield, California. *Geophys. J. Int.* **178,** 1098–1104 (2009).
65. Scholz, C. H. *The Mechanics of Earthquakes and Faulting* 2nd edn (Cambridge Univ. Press, 2003).
66. Kanamori, H. Earthquake physics and real-time seismology. *Nature* **451,** 271–273 (2008).
67. Shibazaki, B. & Iio, Y. On the physical mechanism of silent slip events along the deeper part of the seismogenic zone. *Geophys. Res. Lett.* **30,** 1489 (2003).
68. Liu, Y. & Rice, J. R. Spontaneous and triggered aseismic deformation transients in a subduction fault model. *J. Geophys. Res.* **112,** B09404 (2007).
69. Liu, Y. & Rice, J. R. Slow slip predictions based on granite and gabbro friction data compared to GPS measurements in northern Cascadia. *J. Geophys. Res.* **114,** B09407 (2009).
70. Rubin, A. M. Episodic slow slip events and rate-and-state friction. *J. Geophys. Res.* **113,** B11414 (2008).
71. Segall, P. & Bradley, A. M. Numerical models of slow slip and dynamic rupture including dilatant stabilization and thermal pressurization. *Eos* **90** (suppl.), T22B-08 (2009).
72. Roland, E. & McGuire, J. J. Earthquake swarms on transform faults. *Geophys. J. Int.* **178,** 1677–1690 (2009).
73. Hiramatsu, Y., Watanabe, T. & Obara, K. Deep low-frequency tremors as a proxy for slip monitoring at plate interface. *Geophys. Res. Lett.* **35,** L13304 (2008).
74. Aki, K. Generation and propagation of G waves from the Niigata earthquake of June **16,** 1964, 2, Estimation of earthquake moment, released energy, and stress-strain drop from G wave spectrum. *Bull. Earthq. Res. I. Tokyo* **44,** 73–88 (1966).
75. Kao, H., Wang, K., Dragert, H., Rogers, G. C. & Kao, J. Y. Large contrast between the moment magnitude of tremor and the moment magnitude of slip in ETS events. *Eos* **90** (suppl.), T22B-04 (2009).
76. Chapman, J. S. & Melbourne, T. I. Future Cascadia megathrust rupture delineated by episodic tremor and slip. *Geophys. Res. Lett.* **36,** L22301 (2009).
77. Ide, S., Imanishi, K., Yoshida, Y., Beroza, G. C. & Shelly, D. R. Bridging the gap between seismically and geodetically detected slow earthquakes. *Geophys. Res. Lett.* **35,** L10305 (2008).
78. Ohta, Y., Freymueller, J. T., Hreinsdóttir, S. & Suito, H. A large slow slip event and the depth of the seismogenic zone in the south central Alaska subduction zone. *Earth Planet. Sci. Lett.* **247,** 108–116 (2006).
79. Obara, K. & Hirose, H. Non-volcanic deep low-frequency tremors accompanying slow slips in southwest Japan subduction zone. *Tectonophysics* **417,** 33–51 (2006).
80. Obara, K., Tanaka, S. & Maeda, T. Reevaluation of nonvolcanic tremor activity based on the hybrid method. *Eos* **90** (suppl.), T11C-1835 (2009).
81. Peacock, S. M. & Wang, K. Seismic consequences of warm versus cool subduction metamorphism: Examples from Southwest and Northeast Japan. *Science* **286,** 937–939 (1999).
82. Freed, A. M. Earthquake triggering by static, dynamic, and postseismic stress transfer. *Annu. Rev. Earth Pl. Sc.* **33,** 335–367 (2005).
83. Perfettini, H. & Avouac, J. P. Postseismic relaxation driven by brittle creep: A possible mechanism to reconcile geodetic measurements and the decay rate of aftershocks, application to the Chi-Chi earthquake, Taiwan. *J. Geophys. Res.* **109,** B02304 (2004).
84. Hsu, Y. J. *et al.* Frictional afterslip following the 2005 Nias-Simeulue earthquake, Sumatra. *Science* **312,** 1921–1926 (2006).
85. Savage, J. C. & Yu, S. B. Postearthquake relaxation and aftershock accumulation linearly related after 2003 Chengkung (M6.5, Taiwan) and 2004 Parkfield (M6.0, California) earthquakes. *Bull. Seismol. Soc. Am.* **97,** 1632–1645 (2007).
86. Barbot, S., Fialko, Y. & Bock, Y. Postseismic deformation due to the Mw 6.0 2004 Parkfield earthquake: Stress-driven creep on a fault with spatially variable rate-and-state friction parameters. *J. Geophys. Res.* **114,** B07405 (2009).
87. Marone, C. J. Laboratory-derived friction laws and their application to seismic faulting. *Annu. Rev. Earth Pl. Sc.* **26,** 643–696 (1998).
88. Peng, Z. & Zhao, P. Migration of early aftershocks following the 2004 Parkfield earthquake. *Nature Geosci.* **2,** 877–881 (2009).
89. Vidale, J. E. & Shearer, P. M. A survey of 71 earthquake bursts across southern California: Exploring the role of pore fluid pressure fluctuations and aseismic slip as drivers. *J. Geophys. Res.* **111,** B05312 (2006).
90. Lohman, R. B. & McGuire, J. J. Earthquake swarms driven by aseismic creep in the Salton Trough, California. *J. Geophys. Res.* **112,** B04405 (2007).

91. Nadeau, R. M., Foxall, W. & McEvilly, T. V. Clustering and periodic recurrence of microearthquakes on the San Andreas fault at Parkfield, California. *Science* **267,** 503–507 (1995).
92. Wei, M., Sandwell, D. & Fialko, Y. A silent M_w 4.7 slip event of October 2006 on the Superstition Hills fault, southern California. *J. Geophys. Res.* **114,** B07402 (2009).
93. Wiens, D. A., Anandakrishnan, S., Winberry, J. P. & King, M. A. Simultaneous teleseismic and geodetic observations of the stick–slip motion of an Antarctic ice stream. *Nature* **453,** 770–775 (2008).
94. Schaeffer, D. G. & Iverson, R. M. Steady and intermittent slipping in a model of landslide motion regulated by pore-pressure feedback. *SIAM J. Appl. Math.* **69,** 769–786 (2008).
95. Schulz, W. H., Kean, J. W. & Wang, G. Landslide movement in southwest Colorado triggered by atmospheric tides. *Nature Geosci.* **2,** 863–866 (2009).
96. Ide, S., Beroza, G. C., Shelly, D. R. & Uchide, T. A scaling law for slow earthquakes. *Nature* **447,** 76–79 (2007).
97. Roeloffs, E. A. Evidence for aseismic deformation rate changes prior to earthquakes. *Annu. Rev. Earth Pl. Sc.* **34,** 591–627 (2006).
98. McCausland, W. A., Roeloffs, E. & Silver, P. New insights into Cascadia slow slip events using Plate Boundary Observatory borehole strainmeters. *Eos* **89** (suppl.), G21B-0691 (2008).
99. Perfettini, H., Avouac, J. P. & Ruegg, J. C. Geodetic displacements and aftershocks following the 2001 $M_w = 8.4$ Peru earthquake: Implications for the mechanics of the earthquake cycle along the subduction zones. *J. Geophys. Res.* **109,** B09404 (2005).
100. Rubinstein, J. L., Shelly, D. R. & Ellsworth, W. L. in *Non-volcanic Tremor: A Window into the Roots of Fault Zones, in New Frontiers in Integrated Solid Earth Sciences* (eds Cloetingh, S. & Negendank, J.) 287–314 (Springer, 2010).

Acknowledgements

We thank E. Brodsky, R. McCaffrey, S. Bilek and many others for sharing their measurements of moments and durations of regular earthquakes and slow-slip events. The manuscript benefits from comments by D. Shelly, J. McGuire, K. Obara, T. Melbourne and P. Segall. This work is supported by National Science Foundation (EAR-0809834 and EAR-0956051) and the US Geological Survey.

Author contributions

Both authors have contributed equally to the manuscript.

Additional information

The authors declare no competing financial interests. Supplementary information accompanies this paper on www.nature.com/naturegeoscience.

nature geoscience

SUPPLEMENTARY INFORMATION

DOI: 10.1038/NGEO940

The Supplementary Information includes the following document:

Peng_Gomberg_SuppTable_NGEO_2010.pdf: This table contains the estimates of slip event durations and moments displayed in Figure 5. For each event the table lists the event place name and date, epicentral coordinates, seismic moment and duration, geodetic moment and duration, and the number of the reference from which the information was obtained. The latter number corresponds to the references, with explanatory notes if applicable, listed below the table. Reference numbers also are noted on Figure 5.

DOI: 10.1038/NGEO940

Supplementary Table 1

This table contains the estimates of slip event durations and moments displayed in Figure 5. For each event the table lists the event place name and date, epicentral coordinates, seismic moment and duration, geodetic moment and duration, and the number of the reference from which the information was obtained. The latter number corresponds to the references, with explanatory notes if applicable, listed below the table. Reference numbers also are noted on Figure 5.

Figure 5 Measurements and References

Source Location, Date	Latitude	Longitude	Seismic Moment (N-m)	Seismic Duration (sec)	Geodetic Moment (N-m)	Geodetic Duration (sec)	Ref. No,
Slow Earthquakes							
Mid-Atlantic Ridge 3/20/78	0.90	-29.34	2.400e+18	20.00			1
Prince Edward Islands 8/21/78	-47.48	32.46	5.500e+18	28.00			1
East-Pacific Rise 12/25/78	10.41	-103.80	9.300e+18	28.00			1
Prince Edward Islands 2/18/79	-43.43	41.85	4.900e+18	18.00			1
Mid-Atlantic Ridge 6/10/79	8.17	-38.11	1.600e+18	26.00			1
South of Panama 6/27/79	7.05	-82.40	4.200e+18	36.00			1
Costa Rica 8/24/79	9.02	-83.31	5.800e+18	21.00			1
North-Atlantic Ridge 8/25/79	10.75	-41.70	1.590e+19	34.00			1
North Sumatra 9/29/79	1.23	94.24	2.210e+19	29.00			1
			6.7e+20	200			19
			3.5e+20	80			19
			4e+20	45			19
			3.7e+20	160			19
Kalapana, HI 11/29/75	18.86	-154.95	3.8e+20	72			17
Santa Maria Basin, California 1/31/91	34.8	-120.4	4e+14	3			20
Very Low-frequency Earthquakes							
Shikoku, Japan 3/14/07	33.618	132.357	3.162e+14	17			2
Shikoku, Japan 3/15/07	33.372	132.478	2.239e+14	12			2
Shikoku, Japan 3/15/07	33.436	132.478	6.310e+14	12			2
Shikoku, Japan 3/14/07	33.627	132.514	3.162e+14	18			2

Kii Peninsula, Japan 5/28/06	~34.0	~135.8	1e+15	100			3
Kii Peninsula, Japan 7/18/07	~34.0	~135.8	4.467e+14	70			3
Deep Slow Slip Events (New Zealand)							
Kapiti, 2003					9.5e18	3.154e7	22
Manawatu, 2004					1.72e19	2.938e7	22
Manawatu, 2004					3.07e19	1.642e7	22
Deep Slow Slip Events (Shikoku, Japan)							
1/4/01	33.529	133.004			9.3e+17	691200	4
8/16/01	33.517	132.868			1.01e+18	172800	4
8/18/01	33.720	133.280			8.1e+17	172800	4
2/10/02	33.488	133.169			9.6e+17	432000	4
2/15/02	33.425	132.910			1.14e+18	259200	4
8/6/02	33.438	132.835			6.4e+17	259200	4
8/9/02	33.599	133.125			5.2e+17	345600	4
4/17/03	33.166	132.470			9e+17	345600	4
8/27/03	33.210	132.671			7.6e+17	259200	4
8/30/03	32.370	132.836			1.15e+18	432000	4
11/7/03	33.324	132.922			2.81e+18	518400	4
11/19/03	33.680	133.345			1.05e+18	518400	4
2/10/04	33.170	132.560			1.11e+18	259200	4
4/19/04	33.400	133.020			1.35e+18	604800	4
12/27/04	33.400	132.870			9.3e+17	432000	4
5/12/05	33.284	132.653			1.21e+18	172800	4
5/14/05	33.601	132.930			5.4e+17	345600	4
10/23/05	33.400	132.844			5.1e+17	345600	4
4/15/06	33.451	132.858			1.18e+18	432000	4
9/8/06	33.380	133.030			2.89e+18	777600	4
3/13/07	33.545	132.947			4.7e+17	345600	4
8/27/07	33.629	132.861			5.5e+17	604800	4
9/9/07	33.496	132.861			5.2e+17	259200	4
12/19/07	33.108	132.773			1.99e+18	518400	4
3/13/08	33.467	132.910			8.2e+17	518400	4
11/08/06	34.003	134.293			9.89e+17	259200	4
02/13/08	34.844	134.289			1.35e+18	432000	4
Shallow Slow Slip Event (New Zealand)							
Gisborne, 2002					1e19	864000	22
Gisborne, 2004					7.7e18	1469000	22
Hastings, 2006					6.2e18	777600	22
Gisborne, 2006					5e18	1037000	22
Hastings, 2006					1.33e19	1555000	22
Shallow Creep Event							
Superstition Hills fault, California 10/3/06	32.94	-115.71			1.429e+16	259200	5
Slow or Creep Events							
					4.856e+19	1.581e+7	19
					4.125e+20	1.555e+7	19

DOI: 10.1038/NGEO940

					9e+18	1.728e+6	19
					6e+19	1.261e+8	19
					1.512e+19	2.592e+7	19
					1.26e+16	6.048e+5	19
					1.8e+18	1.728e+6	19
					1.8e+18	5.184e+6	19
					1.134e+19	8.640e+5	19
					7.875e+19	4.709e+7	19
Swarms							
Wooded Island, WA	46.41	-119.28	6.410e+14	1.203e+7	6e+15	1.203e+7	6
Kilauea Volcano, HI 1/26/05	19.30	-155.15	1.8e+14	172800	6.8e+17	190100	7
Kilauea Volcano, HI 1/31/2010	19.30	-155.15			7.943e+17	129600	27
Brawley fault, CA, 1975	32.88	-115.48	4.624e+16	280800			8
West Moreland fault, CA, 1981	33.13	-115.63	6.383e+17	216000			8
Obsidian Buttes fault, CA, 8/29/05	33.17	-115.63	1.023e+17	424800			8
Imperial fault, CA 2003	39.95	-115.55	7.328e+14	64800			8
Galapagos Ridge transform, 2000	1.8	-90.9	9.016e+17	129600			8
Siqueiros transform, 2001	8.3	-103.5	7.586e+17	79200			8
Gofar transform, 2007	-4.6	-105.5	4.786e+16	144000			8
Earthquakes							
Off San Andreas, CA 9/5/04	35.7685	-120.319	3.199e+11	0.056			9
Off San Andreas, CA 9/28/04	35.7784	-120.33	1.429e+13	0.0756			9
Off San Andreas, CA 9/28/04	35.7785	-120.33	2.851e+13	0.0625			9
Off San Andreas, CA 9/28/04	35.7818	-120.323	1.799e+12	0.0778			9
Off San Andreas, CA 9/28/04	35.7771	-120.329	2.851e+13	0.1036			9
Off San Andreas, CA 9/28/04	35.7983	-120.342	1.799e+12	0.0684			9
Off San Andreas, CA 9/29/04	35.7827	-120.334	1.274e+12	0.068			9
Off San Andreas, CA 9/30/04	35.7812	-120.323	4.519e+11	0.0812			9
Off San Andreas, CA 10/7/04	35.781	-120.332	3.589e+12	0.0775			9
Off San Andreas, CA 10/18/04	35.7826	-120.334	1.274e+12	0.0669			9
Off San Andreas, CA 10/18/04	35.7822	-120.334	4.519e+11	0.0596			9
Off San Andreas, CA 10/19/04	35.7699	-120.321	1.799e+12	0.0611			9

Off San Andreas, CA 10/20/04	35.7978	-120.341	5.070e+12	0.07			9
Off San Andreas, CA 10/29/04	35.781	-120.333	1.135e+14	0.0887			9
Off San Andreas, CA 11/3/04	35.7667	-120.318	3.199e+11	0.06			9
Off San Andreas, CA 9/20/01	35.9347	-120.487	2.541e+12	0.0388			9
Off San Andreas, CA 9/28/04	35.9345	-120.487	4.519e+11	0.0392			9
Off San Andreas, CA 9/28/04	35.9347	-120.487	5.070e+12	0.0412			9
Off San Andreas, CA 10/2/04	35.9354	-120.487	7.161e+12	0.0396			9
Off San Andreas, CA 1/8/05	35.9346	-120.487	5.070e+12	0.048			9
Off San Andreas, CA 2/4/04	36.0951	-120.66	1.603e+11	0.044			9
Off San Andreas, CA 2/9/05	36.095	-120.66	1.274e+12	0.0585			9
Off San Andreas, CA 2/9/05	36.0953	-120.66	1.603e+11	0.0516			9
Off San Andreas, CA 3/11/06	36.0362	-120.596	5.248e+12	0.0668			9
Off San Andreas, CA 1/17/07	36.037	-120.595	3.020e+12	0.0607			9
San Andreas fault, CA 6/4/02	35.932	-120.676	3.589e+12	0.0325			9
San Andreas fault, CA 6/4/02	35.932	-120.676	3.589e+12	0.0532			9
San Andreas fault, CA 9/6/04	36.148	-120.653	2.018e+13	0.0924			9
San Andreas fault, CA 9/26/04	36.143	-120.666	4.519e+14	0.1755			9
San Andreas fault, CA 9/27/04	36.154	-120.658	2.018e+13	0.0811			9
San Andreas fault, CA 9/27/04	36.152	-120.658	3.589e+12	0.0788			9
San Andreas fault, CA 10/3/04	36.153	-120.658	2.018e+13	0.074			9
San Andreas fault, CA 6/27/06	36.065	-120.192	7.763e+13	0.1039			9
San Andreas fault, CA 12/15/06	36.17	-120.298	5.248e+12	0.1086			9
San Andreas fault, CA 3/12/07	35.938	-120.691	1.567e+12	0.0256			9
San Andreas fault, CA 9/20/07	36.064	-120.194	3.846e+12	0.1606			9
M7.6 Chi-Chi, Taiwan	23.77	120.98	3.16e+20	28			10

DOI: 10.1038/NGEO940

9/20/99							
M7.1 Hector Mine, CA 10/16/99	34.597	-116.27	5.62e+19	14			11
M7.9 Denali, AK 11/3/02	63.520	147.530	8.91e+20	120			12
M6.5 San Simeon, CA 12/22/03	35.704	- 121.096	7.1e+18	11			13
M6.0 Parkfield, CA 9/28/04	35.815	-120.374	1.3e+18	14			14
Aftershock Sequences							
M6.5 Chengkung, Taiwan 12/10/03	23.065	121.357	6.3e+17	8.64e+7	6.2e+18	8.64e+7	15
M7.9 Denali, AK 11/3/02	63.520	147.530	2.228e+18	8.64e+7			16
M6.0 Parkfield, CA 9/28/04	35.815	-120.374	1e+17	8.64e+7	2.8e+18	8.64e+7	161 5
M7.1 Hector Mine, CA 10/16/99	34.597	-116.27	1.135e+18	8.64e+7			16
M7.6 Chi-Chi, Taiwan 9/20/99	23.77	120.98	1.24e+20	8.64e+7			16
M6.5 San Simeon, CA 12/22/03	35.704	- 121.096	1.2e+17	8.64e+7			16
M6.4 Nima-Gaize, Tibet 1/9/08	32.30	85.32	1.9e+17	6.765e+6	1.17e+18	6.765e+6	23
Landslide							
Mantaro, Peru 4/25/1974	-12.6	-74.6	1.26e+15	240			25
Mount St. Helens, WA 5/18/1980	46.214	-122.194	4e+13	100			26
Glacial Slip							
Dall Glacier, AK 9/2/99	62.66	-152.43	4.027e+16	40			18
Whillans Ice Stream, Antarctica	-84.38	-158.84	1.1e+15	1500	4.9e+19	1500	24

(1) Beroza, G. and Jordan, T. Searching for slow and silent earthquakes using free oscillations. *J. Geophys. Res* **95**, 2485-2510 (1990).

(2) Matsuzawa, T., Obara, K. & Maeda, T. Source duration of deep very-low-frequency earthquakes in western Shikoku, Japan. *J. Geophys. Res.* in press (2010).

(3) Ide, S., Imanishi, K., Yoshida, Y., Beroza, G. C. & Shelly, D. R. Bridging the gap between seismically and geodetically detected slow earthquakes. *Geophys. Res. Lett.* **35**, L10305 (2008).

(4) Sekine, S., Hirose, H. & Obara, K. Along-strike variations in short-term slow slip events in the southwest Japan subduction zone. *J. Geophys. Res.*, in press (2010).

(5) Wei, M., Sandwell, D. & Fialko, Y. A silent Mw4.7 slip event of October 2006 on the Superstition Hills Fault, southern California. *J. Geophys. Res.* **114**, B07402 (2009).
Estimate is based on the statement "more than 27 mm over the next 14 days, with 85% of the amplitude manifested in the first 3 days".

(6) Wicks, C.W., Thelen, W. Weaver, C., Gomberg, J., Rohay, A. and Bodin, P. InSAR observations of aseismic slip associated with an earthquake swarm in the Columbia River basalts, in preparation (2010).

(7) Segall, P., Desmarais, E.K., Shelly, D., Miklius, A. & Cervelli, P. Earthquakes triggered by silent slip on the Kilauea volcano, Hawaii, *Nature* **442**, 71-74, (2006).

(8) Roland, E. & McGuire, J.J. Earthquake swarms on transform faults, *Geophys. J. Int.* **178**, 1677-1690 (2009).

(9) Harrington, R. & Brodsky, E. Source duration scales with magnitude differently for earthquakes on the San Andreas fault and on secondary faults in Parkfield, California. *Bull. Seismol. Soc. Am* **99**, 2323-2334 (2009).

(10) Ma, K.F., Mori, J., Lee, S.J. & Yu, S. B. Spatial and temporal distribution of slip for the 1999 Chi-Chi, Taiwan, earthquake. *Bull. Seismol. Soc. Am.* **91**, 1069-1087 (2001).

(11) Ji, C., Wald, D.J. & Helmberger, D.V. Source description of the 1999 Hector Mine, California, earthquake, Part II: Complexity of slip history. *Bull. Seismol. Soc. Am.* **92**, 1208-1226 (2002).

(12) Ozacar, A.A., Beck, S.L. & Christensen, D.H. Source process of the 3 November 2002 Denali fault earthquake (central Alaska) from teleseismic observations. *Geol. Res. Letts.* **30**, 1638 (2003).

(13) McLaren, M.K., et al. Complex faulting associated with the 22 December 2003 Mw 6.5 San Simeon, California, earthquake, aftershocks, and postseismic surface deformation. *Bull. Seismol. Soc. Am.* **98**, 1659-1680 (2008).
Duration is calculated from an average rupture velocity of 2.8 km/s and a 30 km long fault (length estimated in this paper).

(14) Hartzell, S., Liu, P., Mendoza, C., Ji, C. & Larson, K.M. Stability and uncertainty of finite-fault slip inversions: Application to the 2004 Parkfield, California, earthquake. *Bull. Seismol. Soc. Am.* **97**, 1911-1934 (2007).
Duration calculated from an average rupture velocity of 2.8 km/s and a 40 km long fault (length and rupture velocity estimated in this paper).

(15) Savage, J.C. and Yu, S.B. Postearthquake relaxation and aftershock accumulation linearly related after the 2003 *M* 6.5 Chengkung, Taiwan, and the 2004 *M* 6.0 Parkfield, California, earthquakes. *Bull. Seismol. Soc. Am.* **97**, 1632-1645 (2007).
Aftershock sequence cumulative moments are measured from the plots in Savage et al. (2007) and Savage and Yu (2007) somewhat arbitrarily at 100 days. In all cases, the difference between the moment at 100 days differs insignificantly from that at 1000 days.

(16) Savage, J. C., Svarc, J. L. & Yu, S.B. Postseismic relaxation and aftershocks. *J. Geophys. Res.* **112**, B06406 (2007).

(17) Nettles, M. & Ekstrom, G. Long-period source characteristics of the 1975 Kalapana, Hawaii, earthquake. *Bull. Seismol. Soc. Am.* **94**, 422–429 (2004).

(18) Ekstrom, G., Nettles, M. & Abers, G. Glacial earthquakes. *Science* **302**, 622-624 (2003).

(19) Brodsky, E. E. & Mori, J. Creep events slip less than ordinary earthquakes. *Geophys. Res. Lett.* **34**, L16309 (2007).
The observations in this paper are a compilation from many sources and thus, events are distributed among a variety of tectonic environments, depths, etc. Creep events are those in which slip accrues over days to years and are thus observed geodetically.

DOI: 10.1038/NGEO940

'Tsunami' earthquakes are those that rupture the ocean bottom more slowly than 'fast' earthquakes. 'Fast' earthquakes shown in Figure 3 are not listed in the table because they are too numerous, and all come from only two sources: 1) Abercrombie, R. E. & Rice, J. R. Can observations of earthquake scaling constrain slip weakening? *Geophys. J. Int.* **162**, 406– 424 (2005), and 2) Venkataraman, A., et al. Measurements of spectral similarity for microearthquakes in western Nagano, Japan. *J. Geophys. Res.* **111**, B03303 (2006).

(20) Kanamori, H. & Hauksson, E. A slow earthquake in the Santa Maria Basin, California. *Bull. Seismol. Soc. Am.* **82**, 2087-2096 (1992).

(21) Bilek, S. L., Lay, T. & Ruff, L. J. Radiated seismic energy and earthquake source duration variations from teleseismic source time functions for shallow subduction zone thrust earthquakes. *J. Geophys. Res.* **109**, B09308 (2004).

(22) McCaffrey, R., Wallace, L. & Beavan, J. Slow slip events, temperature and interseismic coupling at the Hikurangi subduction zone, New Zealand. *EOS Trans. Am. Geohys. Union* **88(52)**, Fall Meet. Suppl., Abstract T21A-0367 (2007).

(23) Ryder, J., Burgmann, R. & Sun, J. Tandem afterslip on connected fault planes following the 2008 Nima-Gaize (Tibet) earthquake. *J. Geophys. Res.* **115**, B03404 (2010).

Postseismic deformation (seismic and aseismic) begins after the M5.9 aftershock that occurs 7 days after the mainshock. Postseismic seismic deformation includes only the largest, M5.5 aftershock, although a few M4.9s occurred and the post-seismic deformation is fit with an exponential that has a time constant of 34 days with the duration calculated as the time to reach 90% of the total postseismic slip.

(24) Wiens, D.A., Anandakrishnan, S., Winberry, J.P. & King, M.A. Simultaneous teleseismic and geodetic observations of the stick-slip motion of an Antartic ice stream, *Nature* **453**, 770-774 (2008).

(25) Berrocal, J., Espinosa, A.F. & Galdos, J. Seismological and geological aspects of the Mantaro landslide in Peru. *Nature* **275**, 533-536 (1978).

(26) Kanamori, H. and Given, J. Analysis of long-period seismic waves excited by the May 18, 1980 eruption of Mount St. Helens – A terrestrial monopole? *J. Geophys. Res.* **87**, 5422-5432 (1982).

(27) Poland, M., Mikulius, A., Wilson, D. & Okubo, P. Slow slip event at Kiluea volcano. *EOS Trans. Am. Geophys. Union* **91**, 118-119 (2010).